

Charge Density in Rutile, TiO₂

BY R. RESTORI AND D. SCHWARZENBACH

Institut de Cristallographie, Université de Lausanne, CH-1015 Lausanne, Switzerland

AND J. R. SCHNEIDER

*Hahn–Meitner-Institut für Kernforschung, Glienicker Strasse 100,
D-1000 Berlin 39, Federal Republic of Germany*

(Received 2 September 1986; accepted 16 January 1987)

Abstract

Three high-resolution X-ray data sets of rutile [Ag $K\alpha$ radiation, $(\sin \theta)/\lambda_{\max} = 1.62$ to 1.73 \AA^{-1}] have been measured with three different crystals from two sources at two temperatures, *viz* two synthetic specimens at 295 K and a natural specimen at 100 K. In addition, five low-order Bragg intensities have been measured at 295 K on an absolute scale with γ -ray diffraction. Numerous deformation density refinements have been carried out ($R = 0.59$ to 0.83%) in order to study the effects of data-reduction procedures, extinction corrections, anharmonicity and radial parts of the multipolar deformation functions. Invariant features of the resulting static model deformation maps are (a) residual density maxima of about 0.3 e \AA^{-3} on both types of Ti–O bonds, and (b) a region of negative density at Ti indicating an electron transfer from Ti to O. For one of the crystals, the anisotropy of secondary extinction must be taken into account. The importance of anharmonic effects increases with decreasing temperature, the probability distribution functions of both Ti and O being multimodal at 100 K. This feature might be due to an incipient ferroelectric phase transition, involving a soft transverse-optical phonon mode of symmetry Γ_1^- .

Introduction

The tetragonal ($P4_2/mnm$) structure of rutile, TiO₂, represents one of the simplest and best known structure types. Ti occupies site 2(a), $m. mm, 000, \frac{1}{2} \frac{1}{2} \frac{1}{2}$, and O site 4(f), $m. 2m, \pm(xx0, \frac{1}{2} - x \frac{1}{2} + x \frac{1}{2})$, with $a = 4.593659$ (18), $c = 2.958682$ (8) \AA and $x = 0.30479$ (10) at 298 K (Abrahams & Bernstein, 1971). The coordination of Ti is octahedral with two long apical Ti–O bonds of length 1.9800 (9) \AA , and four short equatorial Ti–O bonds of length 1.9485 (5) \AA . For Ti at 000, the apical bonds are along the twofold axis $\pm[110]$ and the equatorial ones in the mirror plane (110). The TiO₆ octahedra share equatorial edges to form ribbons parallel to [001]. The ribbons are connected through apical corners, resulting in a

planar coordination of O by three Ti atoms, with two Ti–O–Ti angles of $130.60(4)^\circ$ and one Ti–O–Ti angle of $98.79(4)^\circ$. Concerning the physical properties of rutile, we refer to the references given in Abrahams & Bernstein (1971), and Gonschorek (1982).

The experimental determination of the charge density in rutile has been the object of several publications. Shintani, Sato & Saito (1975) were interested in the comparison of the Ti⁴⁺ d^0 ion in rutile with the Ni²⁺ d^8 ion in γ -Ni₂SiO₄. Their difference Fourier map derived from room-temperature Mo $K\alpha$ data at a conventional R value of 0.01 was featureless to within 0.3 e \AA^{-3} , and was interpreted to consist essentially of noise. Gonschorek's (1982, 1983) aim was to find a correlation between the large dielectric constants of rutile and the charge density. He concludes from his room-temperature study using four crystals and Pd-filtered Ag $K\alpha$ radiation that the Ti–O bond is highly covalent. However, the difference Fourier and model deformation maps (Gonschorek, 1983) appear to show important differences between the inequivalent Ti–O bonds, the main density maxima being near the short equatorial ones. The axial bond does not show a density maximum. The reliability indices were relatively high ($R = 0.02$).

Our own research on TiO₂ has been prompted by our interest in the calculation of electric field gradients (EFG) from structure factors (Lewis, Schwarzenbach & Flack, 1982, and references cited therein). Rutile is one of the few compounds for which detailed information of the EFG tensors at all atomic sites is available from nuclear quadrupole resonance spectroscopy using dynamic nuclear polarization (Gabathuler, Hundt & Brun, 1973; Gabathuler, 1974). At the site of O, the sign of the EFG is also known. However, as has been the case in a similarly motivated study of the charge density of cuprite, Cu₂O (Restori & Schwarzenbach, 1986), it turned out that these spectroscopic results cannot be calculated from X-ray data. In compounds with a high heavy-atom content such as TiO₂, the basic question of the feasibility of an experimental charge-density study has not yet been unambiguously

answered. We address in the following this question by identifying common features in difference-density model maps derived from X-ray data sets measured with several crystals at room and low temperature. The role of data-reduction procedures, deformation models, anharmonic-displacement terms and extinction models is also studied.

Experimental, X-rays

Rutile crystals were obtained from two sources. Chemically pure (10 parts in 10^6 Fe) synthetic Verneuil-grown crystals were obtained from the firm Djvahirdjian SA, Monthey, Switzerland. All attempts to prepare spheres from this material with a crystal grinder (Enraf-Nonius) failed. At a diameter of about 0.3 mm, the crystals invariably split along a cleavage plane. A similar experience has been reported by Shintani, Sato & Saito (1975). Therefore, small crystal fragments were chosen with sufficiently well defined faces to permit an adequate absorption correction [$\mu(\text{Ag } K\alpha) = 3.282 \text{ mm}^{-1}$]. In addition, a natural specimen of rutile was used. Scanning electron microprobe analysis showed this to contain about 1% of Fe_2O_3 , essentially localized as inclusions of haematite. From this material, spheres with diameters smaller than 0.2 mm could be prepared easily.

Three data sets were collected with three different crystals (Table 1) on an Enraf-Nonius CAD-4 diffractometer using $\text{Ag } K\alpha$ radiation ($\lambda\alpha_1 = 0.55941 \text{ \AA}$), a nitrogen-gas-flow cooling device and the $2\theta-\omega$ technique. The temperature fluctuations near the nozzle inside the Dewar tube were less than 1 K. All symmetry-equivalent reflections were measured. Backgrounds for crystals 2 and 3 were estimated in two ways: (a) by using the CAD-4 diffractometer program which assumes the first and last sixths of the scan to be background; (b) by applying the minimum $\sigma(I)/I$ criterion (Blessing, Coppens & Becker, 1972). For crystal 1, only (b) was applied. Three intensity control reflections were measured every 3 h. The variance of an intensity was computed according to $\sigma^2(I) = \sigma^2(\text{counting statistics}) + (KI)^2$ where K was obtained from this formula by analysing the fluctuations of the control reflections about their mean values. For the three data sets, $K \approx 0.013, 0.009$ and 0.031 , respectively. The full-sphere ψ -scan data for crystals 1 and 2, collected for $-90 < \psi < 90^\circ$ in steps of 30° , showed considerable intensity fluctuations only for crystal 2, indicating anisotropic extinction effects. Absorption factors and absorption-weighted mean path lengths were computed with Gaussian integration. For the sphere, they were taken from Flack & Vincent (1978). The thermal diffuse scattering (TDS) correction $I_0 = \alpha I(\text{Bragg})$ was evaluated with a program based on Stevens (1974), using the elastic stiffness constants at 298 and 100 K of Manghnani, Fisher & Brower (1972). Unweighted mean values \bar{I} of n symmetry-equivalent

Table 1. *Data collection*

Crystal	1	2	3
Source	Synthetic	Synthetic	Natural
Dimensions (mm)	0.13 × 0.13 × 0.13	0.041 × 0.048 × 0.088	Sphere, 0.18 diam.
Monochromatization	Pd filter	Graphite (002)	LiF (002)
Temperature	295 K	295 K	100 K
Scan angle ω ($^\circ$)	1.40 + 0.45 tan θ	1.30 + 0.45 tan θ	1.30 + 0.45 tan θ
Aperture horizontal ($^\circ$)	0.99 to 1.95	0.99 to 1.95	1.66 to 1.95
Aperture vertical ($^\circ$)	1.32	1.32	1.32
Scan speed ω ($^\circ \text{ min}^{-1}$)	1.0	0.1 to 1.0	0.4 to 1.3
(sin θ)/ λ_{max} (\AA^{-1})*	1.62, 1.41	1.73, 1.62	1.73, 1.62
(sin θ)/ λ_{max} ψ scans (\AA^{-1})	0.76	0.76	—
Number of reflections†	9297, 6957	11380, 8912	8466, —
Number of independent data‡	558, 474	696, 652	701, 661
Absorption, min., max.	1.234, 1.316	1.128, 1.228	1.503, 1.547
TDS, $(1/\alpha)_{\text{min}}$	0.91	0.91	0.97
R(internal), no ψ scans§	0.0203, —	0.0157, 0.0158	0.0193, 0.0192
R(internal), ψ only§	0.0254, —	0.0410, 0.0404	—, —
a, c (\AA)	4.5925 (6), 2.9578 (4)	4.5933 (6), 2.9580 (2)	4.582 (2), 2.953 (1)

* For indices $h+k+l=2n$ and $h+k+l=2n+1$, respectively.

† Including and without ψ -scan data, respectively.

‡ All data and those with $l > 3\sigma(l)$, respectively.

§ Minimum $\sigma(I)/I$ criterion and standard background correction, respectively.

intensities I_i were computed omitting the ψ -scan data. For the variance of \bar{I} , the larger of the two quantities $\sigma_1^2(\bar{I}) = \sum \sigma^2(I_i)/n^2$ and $\sigma_2^2(\bar{I}) = \sum (I_i - \bar{I})^2/n(n-1)$ was chosen.*

All data-reduction calculations were carried out with locally developed programs incorporated in the XRAY72 system (Stewart, Kruger, Ammon, Dickinson & Hall, 1972). The free-atom scattering factors in analytical form and the dispersion corrections were taken from *International Tables for X-ray Crystallography* (1974).

Experimental, γ -rays

The refinement of a scale factor of the X-ray data introduces a major source of error in the charge-density determination. Diffraction experiments with γ -rays allow in principle one to measure structure factors on an absolute scale, and thus to obtain an experimentally determined scale factor (Schneider, Pattison & Graf, 1979; Schneider, 1981). We have therefore measured five low-order structure factors at room temperature on the four-circle γ -ray diffractometer at the Hahn-Meitner Institut. Two wavelengths from neutron-activated ^{192}Ir were used for the experiment, *viz* 0.0392 and 0.0265 \AA . The crystal used was a plane-parallel plate cut from the natural specimen mentioned above. Its thickness was 2.145(5) mm, the surface area 400 mm² and the angle between the plate normal and (010) 2.44°. Surface irregularities were estimated to be smaller than

* Lists of structure factors and deformation parameters have been deposited with the British Library Document Supply Centre as Supplementary Publication No. SUP 43637 (30 pp.). Copies may be obtained through The Executive Secretary, International Union of Crystallography, 5 Abbey Square, Chester CH1 2HU, England.

0.05 mm. Every reflection was measured four times for each of the two wavelengths, namely in two different volume elements and at two ψ angles differing by 1° . Every measurement consisted of an ω step scan of 100 steps with width $\Delta\omega = 0.00625^\circ$. Counting times for each step ranged between 100 and 260 s. The intensity of the primary beam was measured at the start and the end of each series of four ω scans. The intensities were corrected for TDS in analogy to the X-ray data, correction factors ranging from 0.9956 to 0.9999. In view of the short wavelengths, extinction is expected to be small in γ -ray diffraction experiments. A correction derived from Darwin's theory of secondary extinction is therefore considered as sufficient for our present data. The measured integrated reflection power is given by $R_{\text{kin}} \exp(-gR_{\text{kin}})$ where g is inversely proportional to the mosaic spread. The kinematical reflection power R_{kin} is proportional to $|F|^2\lambda^2$. The correction was obtained by extrapolating the structure factors obtained with wavelength λ according to $\ln|F_\lambda| = \ln|F_0| - m\lambda^2$. The results are shown in Table 2.

On the natural crystal plate described above, the intensity of 002 was also measured using a third γ line of ^{192}Ir with $\lambda = 0.0205 \text{ \AA}$ which is much weaker in intensity. In addition, a similar plane-parallel plate was prepared from the synthetic crystal and used for three more measurements of 002 with all three wavelengths. The results do not agree well with the data of Table 2. The structure factors at 0.0205 \AA are too low in comparison with the other wavelengths, and extinction effects appear to be more important for the synthetic specimen. With all data taken into account, $|F(002)|^2$ lies in the rather broad interval from 1391 to $1436e^2$, i.e. $37.3e < |F(002)| < 37.9e$. However, $|F_0|^2$ is not determined to better than 1% even if only the data of Table 2 are accepted. This somewhat disappointing result might be due to the mediocre quality of the crystals. High-resolution rocking curves of 002 (Schneider & Graf, 1986) indicated the mosaic distributions to be irregular. They showed asymmetric maxima for the natural crystal, and many distinct sharp maxima for the synthetic crystal. A more detailed description of the γ -ray experiments is given by Restori (1986).

Charge-density refinements

The charge-density refinement program *LSEXP* has been described by Restori & Schwarzenbach (1986). In the present work, the following options were used:

(a) Secondary extinction according to Becker & Coppens (1974, 1975). The general isotropic correction was refined for all three data sets and included two variables, G for the spread of the Lorentzian mosaic distribution and R for the domain size. For data set 2, anisotropic extinction was also refined using seven variables, viz a second-rank tensor for

Table 2. Room-temperature structure factors from γ -ray diffraction

$|F_\lambda|^2$ = mean value of $n=4$ measurements; $|F_0|^2$ = extinction-corrected value; $\sigma_1 = \sigma/n^{1/2}$, σ = e.s.d. of an individual intensity from counting statistics and the e.s.d.'s of various correction factors; σ_2 = e.s.d. from the deviations of individual intensities from the mean.

<i>hkl</i>	$\lambda = 0.0392 \text{ \AA}$			$\lambda = 0.0265 \text{ \AA}$			$ F_0 ^2$
	$ F_\lambda ^2$	σ_1	σ_2	$ F_\lambda ^2$	σ_1	σ_2	
002	1312.0	6.2	7.5	1369.7*	9.8	4.2	1420.3
301	958.8	5.3	4.1	992.6*	8.0	2.7	1021.9
101	512.5	2.8	1.3	532.1	4.2	2.2	549.2
400	382.5	3.1	4.7	387.5	4.4	6.9	391.7
004	319.0	3.0	5.1	319.3	4.9	3.4	319.6

* $n = 3$.

the Lorentzian mosaic distribution (Thornley & Nelmes, 1974) and one variable for the domain size. Corresponding refinements are identified with the codes *I* and *A*, respectively.

(b) Refinements using structure amplitudes obtained with the standard background correction, and with the minimum $\sigma(I)/I$ criterion are identified by *N* and *L*, respectively.

(c) Third- and fourth-order anharmonic displacement parameters are represented by the Gram-Charlier series expansion formalism (Johnson & Levy, 1974). This adds six variables for Ti and nine for O. Harmonic and anharmonic refinements are identified with *H* and *G*, respectively.

(d) Aspherical atoms are represented by a sum of multipolar deformation functions

$$\rho_{nlm\pm} = P_{nlm\pm} \rho_n(r) C_{lm\pm} Y_{lm\pm}$$

(Stewart, 1976) which are exactly equivalent to the deformation functions of Hirshfeld (1977). For Ti and O, three monopolar ($n=0, 2, 4$), two sets of quadrupolar ($n=2, 4$) and one set of hexadecapolar ($n=4$) functions were used. In addition, two dipolar ($n=1, 3$) and one set of octopolar ($n=3$) functions were assigned to O, resulting in 10 and 14 population parameters $P_{nlm\pm}$ for Ti and O, respectively [indexing rules of site symmetric spherical harmonics are given by Kurki-Suonio (1977)]. The radial functions were represented either by $\rho_n = N_n r^n \exp(-\alpha r)$, or for $n=l$ by Lorentzians $\rho_n = N'_n x^n / (1+x^2)^{n+2}$, $x = r/\beta$. $C_{lm\pm}$, N_n and N'_n are normalization constants, and α and β are refinable parameters. Refinements using only exponential functions are identified by *E*, those also using Lorentzians by *M* (mixed basis). The spherical-atom (procrystal) model is identified by *P*.

All full-matrix refinements were with respect to $|F|^2$, with weights equal to the inverse of the variance of $|F|^2$. The highest-order reflections showed for all refinements an increase of the weighted differences $w(|F_0|^2 - |F_c|^2)^2$ which could not be accounted for by anharmonic displacement terms. For many of these reflections, backgrounds were abnormally high, or

Table 3. Harmonic displacement parameters and reliability indices

Definitions: $S = [\sum w(|F_o|^2 - |F_c|^2)/(n - m)]^{1/2}$, $n - m$ = number of degrees of freedom; $R = \sum \|F_o| - |F_c|/\sum |F_o|$. U 's are 10^{-5} \AA^2 ; e.s.d.'s are given in parentheses; the temperature-factor expression is $\exp[-2\pi^2 \sum U_{ij} a_i^* a_j^* h_i h_j]$; the eigenvalues are $U(110) = U_{11} + U_{12}$ parallel to Ti-O bond, $U(\bar{1}10) = U_{11} - U_{12}$, $U(001) = U_{33}$. I/A = isotropic/anisotropic extinction, N/L = standard background treatment/minimum $\sigma(I)/I$; H/G = harmonic displacement parameters/Gram-Charlier expansion; E/M = exponential/mixed basis: P = spherical atoms; 1, 2, 3 identify the data sets.

	[110]		$\bar{1}10$		[001]		S	R	S	R
	$U(\text{Ti})$	$U(\text{O})$	$U(\text{Ti})$	$U(\text{O})$	$U(\text{Ti})$	$U(\text{O})$				
1ILHP	689 (5)	365 (8)	709 (5)	768 (9)	493 (2)	445 (6)	1.77	0.01061	—	—
1ILHE	701 (4)	389 (6)	727 (4)	797 (8)	510 (3)	466 (6)	1.04	0.00828	1.03	0.00807
1ILHM	690 (3)	371 (5)	716 (3)	780 (6)	499 (2)	447 (4)	1.05	0.00827	1.02	0.00793
2INHP	717 (4)	388 (6)	737 (4)	784 (7)	523 (2)	469 (4)	2.88	0.00982	—	—
2INHE	716 (1)	388 (2)	737 (1)	784 (3)	523 (1)	466 (2)	1.15	0.00643	1.12	0.00630
2INHM	715 (1)	387 (2)	737 (1)	784 (3)	523 (1)	467 (2)	1.12	0.00642	1.11	0.00628
2ILHE	708 (1)	385 (2)	728 (1)	780 (3)	516 (1)	461 (2)	1.32	0.00686	1.25	0.00651
2ILHM	707 (1)	382 (2)	729 (1)	780 (3)	515 (1)	462 (2)	1.28	0.00664	—	—
2ALHE*	708 (1)	388 (2)	730 (1)	787 (3)	517 (1)	465 (2)	1.36	0.01505	1.36	0.01491
2ALHM*	709 (1)	389 (2)	731 (1)	787 (3)	518 (1)	465 (2)	1.37	0.01510	1.36	0.01492
3INHP	356 (2)	254 (4)	362 (2)	442 (5)	259 (1)	302 (3)	1.81	0.00968	—	—
3INHE	365 (2)	268 (3)	369 (2)	458 (4)	273 (2)	318 (3)	1.17	0.00673	1.10	0.00615
3INHM	355 (2)	257 (3)	361 (2)	445 (3)	267 (2)	306 (2)	1.19	0.00664	1.10	0.00610
3ILHE	370 (2)	272 (3)	373 (2)	464 (4)	277 (2)	323 (3)	1.20	0.00639	1.12	0.00587
3ILHM	362 (2)	262 (2)	366 (2)	455 (3)	272 (2)	310 (2)	1.21	0.00645	1.13	0.00590

* Non-averaged data set.

unequal to the left and right of the peak. A similar effect has been observed for Cu_2O (Restori & Schwarzenbach, 1986). The physical reasons remain unexplained, but may be connected with the geometry of the CAD-4 instrument. The maximal $(\sin \theta)/\lambda$ was subsequently limited to 1.55, 1.65 and 1.60 \AA^{-1} in the refinements of data sets 1, 2 and 3, respectively. As for Cu_2O , convergence of the refinements was considered complete at full shift/e.s.d. values for all parameters smaller than 10^{-4} . At no stage was the physical reasonableness of the resulting values of the variables tested. The different models served only to parametrize the data. In fact, individual deformation or anharmonic displacement parameters may not possess physical significance. Reliability indices and harmonic-displacement parameters are given in Table 3. In addition, the range of values obtained for several quantities are for data sets 1, 2 and 3, respectively: weighted R value $wR(|F^2|)$ for the spherical-atom procrystal model P 0.02194, 0.03077 and 0.02133; $wR(|F^2|)$ for the deformation models 0.01255 to 0.01260, 0.01171 to 0.01380 (isotropic extinction) and 0.01350 to 0.01385; smallest extinction correction y_{\min} ($F_o = \text{scale} \times y \times F_{\text{corr}} = \text{scale} \times F_c$) 0.84 to 0.86, 0.81 to 0.91 and 0.88 to 0.94; scale factor 23.66 to 24.50, 18.43 to 18.98 and 37.44 to 38.67. There is no systematic trend in the reliability indices permitting one to prefer background corrections N or L , or radial bases E or M . For the room-temperature data sets 1 and 2, the anharmonic models G do not result in an appreciably better fit with observations than the harmonic models H . Surprisingly, for the low-temperature data set 3, anharmonic effects appear to be more important, as evidenced by the lowering of S and R in going from H to G .

The structure amplitudes $|F_\gamma|$ from γ -ray diffraction give additional information on the scale factor and the extinction parameters. They are related to the X-ray structure amplitudes $|F_X|$ by

$$|F_X| = \text{scale} \times y_{\text{ext}}(G, R) \times |F_\gamma|,$$

where y_{ext} is the extinction correction. Estimates of scale, G and R can be obtained by a least-squares fit. However, in subsequent charge-density refinements with respect to $|F_X|^2$, the resulting values should not be kept fixed. Rather, they should be restrained with slack constraints using weights equal to the inverse of their variances. We have adopted an equivalent but more efficient procedure by introducing $|F_\gamma|^2$ together with all X-ray data in the charge-density refinements of the room-temperature data sets 1 and 2. If the weights are $w = \sigma^{-2}$, σ being the larger of the two quantities σ_1 and σ_2 (Table 2), the effect of the γ -ray data is small. In refinement 1ILHE, for example, the scale factor decreases by 1.7% from 24.29(16) to 23.88(6), the extinction remains nearly constant, the R value increases from 0.828 to 0.882% and the goodness-of-fit S from 1.04 to 1.11. Positional and displacement parameters fall into the range of values obtained with the X-ray data alone (Table 3). The corresponding charge-density map is almost indistinguishable from Fig. 2(a). The $w^{1/2}(|F_\gamma|^2 - |F_c|^2)$ values decrease nearly linearly with $(\sin \theta)/\lambda$ from 2.5 for 101 to -3.4 for 004. Similar results were obtained with other charge-density models. The γ -ray data thus agree reasonably well, but not completely, with the X-ray data. They are not of sufficient precision to counterbalance the large number of X-ray data and do not add much new significant information. On the other hand, refinements with the weights

of $|F_{\gamma}|^2$ increased by a factor of 100 show that γ -ray data with an accuracy of 0.1 to 0.2% would modify the results significantly. It should also be remembered that the γ -ray and X-ray measurements at room temperature were made on different crystals.

Results and discussion

(a) Standard structural parameters

For the room-temperature data sets 1 and 2, the positional parameter x of O varies between 0.30471 (6) and 0.30493 (3) with a mean value of 0.30485. This is in very good agreement with the references cited above. At 100 K, x varies between 0.30472 (5) and 0.30475 (3) with a mean of 0.30473. The long Ti–O distance decreases by only 0.005 (1) Å, and the short one by 0.003 (1) Å in going from 295 to 100 K.

The harmonic-displacement parameters of crystals 1 and 2 (Table 3) agree reasonably well, the standard deviation computed from $[\sum(U - \langle U \rangle)^2/7]^{1/2}$ being 6 to 8×10^{-5} Å². They are, however, larger by about 0.0006 Å² than the published X-ray and neutron results (Gonschorek & Feld, 1982). This discrepancy is due to our TDS correction. Spherical-atom refinements using our data not corrected for TDS are in good agreement with the previous determinations. In addition, our results and all previous ones show the same characteristic peculiarities:

The U 's of O agree with intuition. The largest one is along $[\bar{1}10]$ perpendicular to the plane of the O–Ti bonds, and the smallest one is along $[110]$ parallel to the long O–Ti bond. The U 's of Ti, on the other hand, are anomalously large, as evidenced by the mean-square displacements (m.s.d.'s) along the Ti–O bonds. At 295 K, the m.s.d.'s of Ti and O calculated from the mean $\langle U \rangle$'s are 0.00707 and 0.00385 Å² along the long and 0.00606 and 0.00429 Å² along the short bond, respectively. Corresponding values at 100 K are 0.00363, 0.00265 Å², and 0.00312, 0.00293 Å². Thus, the anomaly persists even at low temperature. The bonds appear to be non-rigid, and the heavier atom shows the larger displacements.

(b) Anharmonicity

For the anharmonic displacement parameters, values up to 7.6 e.s.d.'s were obtained at 100 K. Fig. 1 shows the probability density functions (p.d.f.'s) of Ti and O at 100 K, calculated according to Johnson & Levy (1974). Surprisingly, the anharmonic p.d.f.'s are bimodal in the directions where the harmonic U 's are *smallest*, viz $[001]$ for Ti, and $[001]$ and $[110]$ for O. The largest probability density of O in the plane $(\bar{1}10)$ is located on an approximate circle of radius 0.06 Å centered on the mean atomic position. The p.d.f.'s in the directions where the harmonic U 's are *largest*, namely $[110]$ and $[\bar{1}10]$ for Ti and $[\bar{1}10]$ for

O, are unimodal and rather diffuse. Similar p.d.f.'s are found for all anharmonic models of data set 3. We do not possess another low-temperature data set from a different crystal or from the literature to confirm these findings. The anharmonic p.d.f. of Ti from data set 1 might, however, be considered as corroborating but weak evidence. It resembles Fig. 1, with the peak of the $[001]$ curve flattened into a plateau of slightly increasing probability from 0.0 to 0.06 Å. Data set 2 does not show this effect.

Rutile has been described as an incipient ferroelectric, possessing two transverse-optical phonon modes whose frequencies *decrease* strongly with *decreasing* temperature (Samara & Peercy, 1973; Gervais & Kress, 1983). The $A_{2u}(\Gamma_1^-)$ soft mode at wavevector zero is polar and consists of displacements of Ti with respect to the oxygen framework along $[001]$. The deviations of the p.d.f.'s from a Gaussian shape should thus indeed *increase* with *decreasing* temperature. Our results would then indicate an oscillation between the two orientations $\pm[001]$ of a ferroelectric structure. A displacement of all Ti atoms along $[00\bar{1}]$ with respect to the center of mass of the unit cell implies a displacement of O in the opposite direction $[001]$. This movement would tend to increase the short distance of 2.531 Å between the O atoms at $xx0$ and $1-x\ 1-x\ 0$, forming the common edge between adjacent octahedra. The probable displacement of O at $xx0$ would thus be towards $x - \mu x - \mu v$, resulting in a multimodal p.d.f. in the plane $(\bar{1}10)$, in agreement with Fig. 1. More information on this mode could be obtained with an accurate high-resolution neutron data set at very low temperatures.

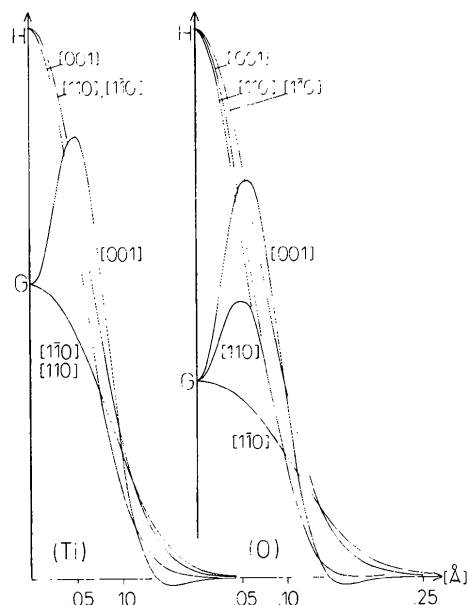


Fig. 1. Probability density functions at 100 K, refinements 31NHM and 31NGM. The p.d.f. of Ti, and the p.d.f. of O along $[001]$ and $[\bar{1}10]$ are even functions. Along $-\bar{1}10$, the p.d.f. of O is 1 to 3% lower than along $+\bar{1}10$.

(c) Model maps

Figs. 2 to 4 show a selection of static model deformation-density maps, obtained by summation of the deformation functions in direct space. Standard deviations have been estimated by summing the variances and covariances of the deformation parameters (Hirshfeld, 1977). More maps can be found in Restori (1986).

Both Ti-O bonds show residual electron density for data sets 1 and 3. These bond maxima have heights of 0.25 to $0.30 \text{ e } \text{Å}^{-3}$ and are clearly separated on *all* maps from the refinements of data set 3 (Fig. 4). The two short bonds, related by the mirror plane (001) parallel to the long bond, are connected by a bridge of diffuse density of $0.1 \text{ e } \text{Å}^{-3}$. In the maps of data set 1, this bridge becomes a banana-shaped feature of constant density, while the maximum on the long bonds is still resolved (Fig. 2). If in these refinements γ -ray data are used with weights 100 times larger than the inverse of their variances, the maxima become again resolved, and increase in height. But near Ti, very sharp features are then introduced which resemble those of Fig. 2(b). As mentioned before, the

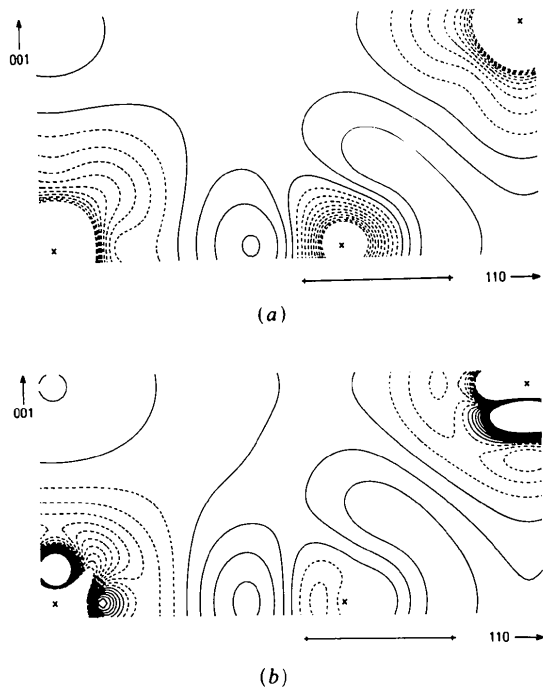


Fig. 2. Static model deformation maps at infinite resolution in the plane $(\bar{1}10)$, data set 1, 295 K. Interval $0.1 \text{ e } \text{Å}^{-3}$, zero and positive contours full lines, negative contours broken. E.s.d.'s at distances larger than 0.5 Å from the atomic centres are $0.05 \text{ e } \text{Å}^{-3}$; near the atoms, they are very model dependent, i.e. large for steep features and small for flat features. The orientations of the Ti atoms at 000 (lower left) and $\frac{1}{2} \frac{1}{2} \frac{1}{2}$ (upper right) differ by a rotation of 90° around $[001]$; a mirror line runs parallel to the long Ti-O bond through Ti at 000 and O at $xx0$; the short bonds are between $xx0$ and $\frac{1}{2} \frac{1}{2} \pm \frac{1}{2}$. (a) Refinement 11LHE. (b) Refinement 11LGM.

γ -ray data have no perceptible effect on the maps if they are weighted according to their variances. The maps of data set 2 (Fig. 3) obtained with isotropic extinction show resolved peaks on the short bonds, but no density on the long bond. The agreement factors of Table 1 indicate that the ψ -scan data of this crystal show relatively large intensity fluctuations.

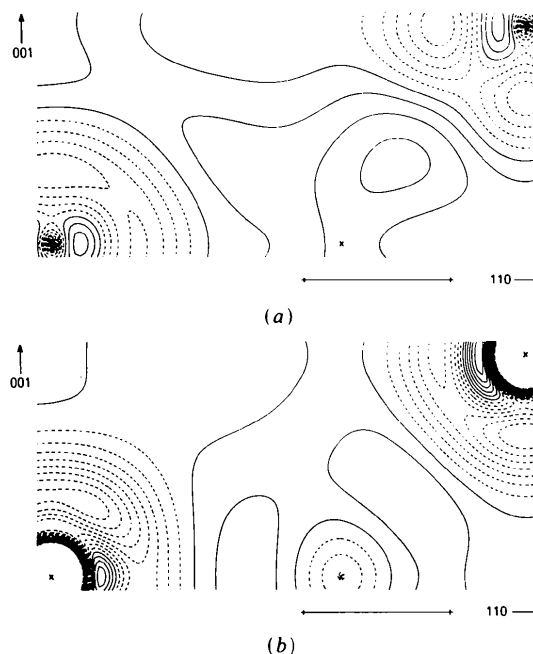


Fig. 3. Static model deformation maps, data set 2, 295 K. (a) Refinement 21LHE. (b) Refinement 2ALGE.

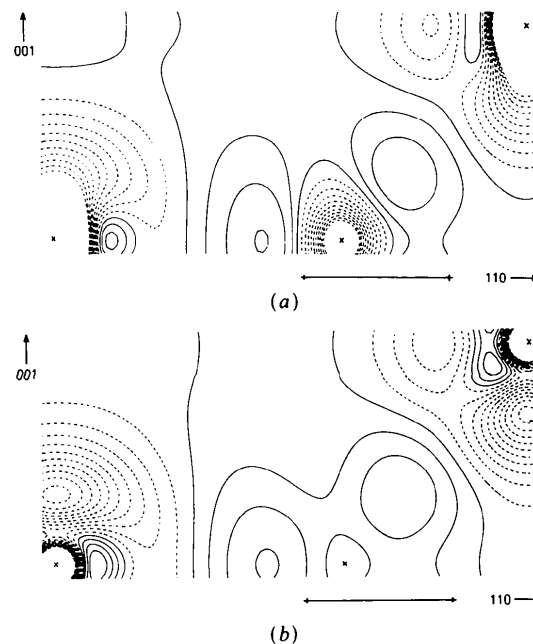


Fig. 4. Static model deformation maps, data set 3, 100 K. (a) Refinement 31NHE. (b) Refinement 31NGM.

This might be explained by anisotropic extinction effects. The maps resulting from the refinements 2A... resemble indeed those from data set 3, except that the densities are lower. This illustrates the bias due to inappropriate extinction models.

The region of Ti is always characterized by negative density, usually elongated along [001]. A maximum might appear on the long bond at 0.4 Å from Ti whose height varies considerably with the model used. It is more pronounced for the mixed basis *M*, but there appears to be no correlation with the choices of *H* vs *G* and *N* vs *L*. At the site of O, the basis *E* results in strongly negative densities (except for data set 2) while *M* gives densities near zero. Maps drawn in the plane (001) through Ti and O do not show additional features, and in particular no densities near O which could be attributed to lone-pair electrons.

The following features of the charge density, present on all or most maps, are probably significant and represent the physical reality:

(a) bonding peaks of about $0.3 \text{ e } \text{Å}^{-3}$ on all Ti-O bonds;

(b) negative electron density near Ti, elongated towards the nearest Ti neighbors.

The electron densities of rutile and corundum, Al_2O_3 (Lewis, Schwarzenbach & Flack, 1982) show certain similarities. Both show an electron transfer from the metal to the oxygen, the latter being polarized along the bonds. Symmetrically inequivalent bonds of different lengths show nearly identical features. TiO_2 and Al_2O_3 are both derived from an h.c.p. arrangement of O, with d^0 cations occupying octahedral voids. Their physical properties, on the other hand, and in particular hardness and refractive indices, are very dissimilar. Evidently, the electron density is not a quantity sensitive to these properties. There exists also an important difference between bonds formed by d^0 cations and bonds involving *d* electrons, the latter showing little residual density on the bond axis (Coppens, 1985), or even a strongly negative density as found in Cu_2O (Restori & Schwarzenbach, 1986). As was the case for Cu_2O , the electric field gradients calculated from the deformation functions are extremely model dependent and cannot be related to the experimental ones.

This work is part of a PhD thesis (Restori, 1986). The calculations were carried out at the computer center of the Swiss Federal Institute of Technology at Lausanne (CDC Cyber 170-855). The project is

supported by the Swiss National Science Foundation, grant 2.270-0.84.

References

- ABRAHAMS, S. C. & BERNSTEIN, J. L. (1971). *J. Chem. Phys.* **55**, 3206-3211.
- BECKER, P. J. & COPPENS, P. (1974). *Acta Cryst.* **A30**, 129-147.
- BECKER, P. J. & COPPENS, P. (1975). *Acta Cryst.* **A31**, 417-425.
- BLESSING, R. H., COPPENS, P. & BECKER, P. J. (1972). *J. Appl. Cryst.* **7**, 488-492.
- COPPENS, P. (1985). *Coordination Chemistry Reviews*, Vol. 65, pp. 285-307. Amsterdam: Elsevier.
- FLACK, H. D. & VINCENT, M. G. (1978). *Acta Cryst.* **A34**, 489-491.
- GABATHULER, CH. (1974). *Dynamische Kernpolarisation in Rutil*. PhD Thesis, Univ. of Zürich, Switzerland.
- GABATHULER, CH., HUNDT, E. E. & BRUN, E. (1973). *Proc. XVII Congress Ampere*, edited by V. HOVI. Amsterdam: North-Holland.
- GERVAIS, F. & KRESS, W. (1983). *Phys. Rev. B*, **28**, 2962-2968.
- GONSHOREK, W. (1982). *Z. Kristallogr.* **160**, 187-203.
- GONSHOREK, W. (1983). *Die räumliche Verteilung der Bindungselektronen im Rutil (TiO₂) untersucht mit Beugungsmethoden*. Habilitationsschrift, Technische Hochschule Aachen, Federal Republic of Germany.
- GONSHOREK, W. & FELD, R. (1982). *Z. Kristallogr.* **161**, 1-5.
- HIRSHFELD, F. L. (1977). *Isr. J. Chem.* **16**, 226-229.
- International Tables for X-ray Crystallography* (1974). Vol. IV. Birmingham: Kynoch Press. (Present distributor D. Reidel, Dordrecht.)
- JOHNSON, C. K. & LEVY, H. A. (1974). *International Tables for X-ray Crystallography*, Vol. IV, pp. 314-319. Birmingham: Kynoch Press. (Present distributor D. Reidel, Dordrecht.)
- KURKI-SUONIO, K. (1977). *Isr. J. Chem.* **16**, 115-123.
- LEWIS, J., SCHWARZENBACH, D. & FLACK, H. D. (1982). *Acta Cryst.* **A38**, 733-739.
- MANGHNANI, M. H., FISHER, E. S. & BROWER, W. S. (1972). *J. Phys. Chem. Solids*, **33**, 2149-2159.
- RESTORI, R. (1986). *Densité Electronique Expérimentale dans des Structures Simples: Influence du Modèle*. PhD Thesis, Univ. of Lausanne.
- RESTORI, R. & SCHWARZENBACH, D. (1986). *Acta Cryst.* **B42**, 201-208.
- SAMARA, G. A. & PEERCY, P. S. (1973). *Phys. Rev. B*, **7**, 1131-1148.
- SCHNEIDER, J. R. (1981). *Nuclear Science Applications*, Vol. 1, pp. 227-276. New York: Harwood Academic Publishers.
- SCHNEIDER, J. R. & GRAF, H. A. (1986). *J. Cryst. Growth*, **74**, 191-202.
- SCHNEIDER, J. R., PATTISON, P. & GRAF, H. A. (1979). *Nucl. Instrum. Methods*, **166**, 1-19.
- SHINTANI, H., SATO, S. & SAITO, Y. (1975). *Acta Cryst.* **B31**, 1981-1982.
- STEVENS, E. D. (1974). *Acta Cryst.* **A30**, 184-189.
- STEWART, J. M., KRUGER, G. J., AMMON, H. L., DICKINSON, C. W. & HALL, S. R. (1972). *The XRAY72 System*. Tech. Rep. TR-192. Computer Science Center, Univ. of Maryland, College Park, Maryland.
- STEWART, R. F. (1976). *Acta Cryst.* **A32**, 565-574.
- THORNLEY, F. R. & NELMES, R. J. (1974). *Acta Cryst.* **A30**, 748-757.